Pharmacological Research 159 (2020) 104991

Contents lists available at ScienceDirect

Pharmacological Research

journal homepage: www.elsevier.com/locate/yphrs

LSD1 deletion represses gastric cancer migration by upregulating a novel miR-142-5p target protein CD9

Li-Juan Zhao, Qi-Qi Fan, Ying-Ying Li, Hong-Mei Ren, Ting Zhang, Shuan Liu, Mamun Maa, Yi-Chao Zheng*, Hong-Min Liu*

State Key Laboratory of Esophageal Cancer Prevention & Treatment, Key Laboratory of Advanced Drug Preparation Technologies, Ministry of Education of China, Collaborative Innovation Center of New Drug Research and Safety Evaluation, Henan Province, Key Laboratory of Henan Province for Drug Quality and Evaluation, Institute of Drug Discovery and Development, School of Pharmaceutical Sciences, Zhengzhou University, 100 Kexue Avenue, Zhengzhou, Henan 450001, China

ARTICLE INFO

Keywords:
LSD1
miR142-5p
CD9
Gastric cancer
Migration
Small extracellular vesicles

ABSTRACT

LSD1 (histone lysine specific demethylase 1) takes part in the physiological process of cell differentiation, EMT (epithelial-mesenchymal transition) and immune response. In this study, we found LSD1 expression in metastatic gastric cancer tissues was significantly higher than that in normal tissues. Furthermore, LSD1 deletion was found to suppress gastric cancer migration by decreasing intracellular miR-142 − 5p, which further led to the upregulation of migration suppressor CD9, a newly identified target of miR-142 − 5p. While LSD1 was reported as a demethylase of H3K4me1/2, H3K9me1/2 and several non-histone proteins, this is a new evidence for LSD1 as a functional regulator of miRNA. On the other hand, our data suggested that promoting the secretion of miR-142 − 5p using small extracellular vesicles as vehicles is a new mechanism for LSD1 abrogation to down-regulate intracellular miR-142 − 5p. Taken together, this study uncovered a new mechanism for LSD1 that can contribute to gastric cancer migration by facilitating miR-142 − 5p to target CD9.

1. Introduction

GC (Gastric cancer) is the fifth most frequently diagnosed cancer worldwide and the third leading cause of cancer death as it is responsible for over 1,000,000 new cases in 2018 and an estimated 783,000 deaths (equal to 1 in every 12 deaths globally) [1]. In addition, GC patients usually perform poor prognosis, with a reported five-year survival rate less than 10 percent [2], and one of the main contributors to the poor survival rate is the high metastasis rate at the time of diagnosis. Consequently, identification of key participant in the metastatic progression of GC, and understand the mechanism for GC metastasis may provide promising therapeutic remedies.

LSD1 is the first identified histone lysine demethylase in 2004 [3], as an eraser of H3K4me1/2 and H3K9me1/2 as well as some non-histone substrates methylation [4], and overexpression of LSD1 has been reported as a driver in several kinds of cancers [5–7]. In the past decades, more and more evidence indicated that LSD1 participated in cancer progression and embryonic development as an epigenetic regulator of transcription [8–13]. However, its impact on ncRNAs (non-coding RNAs) has not been studied until Yang Shi reported that decreased expression of LSD1 contributes to dsRNA (double strand RNA) stress and promotes IFN (interferon) activation by down regulating the expression of RISC (RNA-induced silencing complex) components [14], which include Dicer (a member of RNase III family that specifically cleaves double-stranded RNAs to generate miRNAs (microRNAs) [15] and AGO2 (Argonaute RISC Catalytic Component 2, a participant in miRNA-mediated gene silencing as a translational repressor) [16][13]. So, LSD1 has the potential to regulate miRNA generation, but whether miRNA is involved in the LSD1 mediated oncogenesis remains to be answered.

MiRNAs are short RNA molecules with 19–25 nucleotides that negatively regulate gene expression post-transcriptionally by base pairing on target mRNAs [17–19]. Primary miRNAs (pri-miRNAs) are precursors of miRNAs that are transcribed by RNA polymerase II, and then

Abbreviations: LSD1, Histone lysine specific demethylase 1; GC, Gastric cancer; EMT, Epithelial-mesenchymal transition; RISC, RNA-induced silencing complex; AGO2, Argonaute RISC Catalytic Component 2; ncRNAs, Non-coding RNAs; dsRNA, Double strand RNA; IFN, Interferon; pri-miRNAs, Primary miRNAs; pre-miRNAs, Precursor miRNAs; miRISC, miRNA-induced silencing complex; EVs, Extracellular vesicles; sEVs, Small extracellular vesicles; MVB, Multivesicular bodies; TEM, Transmission electron microscope; NTA, Nanoparticle tracking analysis; UC, Ultracentrifugation; KO, Knockout; HE staining, Hematoxylin-eosin staining; IHC, Immunohistochemistry; RPMI 1640, Roswell Park Memorial Institute 1640; RIPA, Radio immunoprecipitation assay; PBS, Phosphate buffer saline

* Corresponding authors.
E-mail addresses: yichaozheng@zzu.edu.cn (Y.-C. Zheng), liuhm@zzu.edu.cn (H.-M. Liu).

https://doi.org/10.1016/j.phrs.2020.104991
Received 3 March 2020; Received in revised form 25 April 2020; Accepted 31 May 2020
Available online 03 June 2020

pri-miRNAs are processed into hairpin precursor miRNAs (pre-miRNAs) by nuclear RNase Drosha. When pre-miRNA is transported into the cytoplasm, where the pre-miRNA interacts with Dicer, the hairpin is cleaved off, resulting in double-stranded mature miRNA [20]. Following this, the RNA duplex is released and one strand is integrated into argonaute protein containing miRISC (miRNA-induced silencing complex) and interacts with target miRNA transcripts, which leads to the repression of gene expression [21]. Therefore, the level of intracellular miRNA is mainly regulated by this synthetic pathway. On the other hand, sEVs (small extracellular vesicles) are vesicles derived from cells, which revolutionize our understanding of cell-to-cell communication [22], and are capable to not only load small RNAs, proteins, DNA and lipids, release them out of cells, but also deliver them to recipient cells [23]. Thus, miRNAs packaged into sEVs could serve as a new and unique model to understand the dysregulated content of intracellular miRNA.

In this study, LSD1 was found to promote GC metastasis by acting as a positive upstream regulator of miR-142−5p, which contributed to GC metastasis by degrading CD9 mRNA, a novel target of miR-142−5p. Furthermore, abrogation of LSD1 promoted miR-142−5p to be packaged into sEVs, which served as a cooperate mechanism for LSD1 to regulate intracellular miR-142−5p. Our findings point to the new pathway for LSD1 to accelerate GC metastasis, which will contribute to understand the mechanism about the regulation of LSD1 on GC metastasis.

2. Materials & methods

2.1. Cell culture

Gastric cancer cell lines MGC-803, AGS and HEK293 T (human embryonic kidney 293 T) cell line were purchased from Cell Bank of the Chinese Academy of Sciences (Shanghai, China). MGC-803 and AGS cells were maintained in RPMI-1640 Medium (01−100-1ACS, BioInd, Israel). HEK293 T cells were maintained in DMEM medium (01−052-1ACS, BioInd, Israel). The medium was supplemented with 10 % FBS (Fetal bovine serum, 04−001-1A, BioInd, Israel). All cells were grown in a humidified atmosphere of 5% CO_2 at 37 ˚C.

2.2. LSD1 KO cell models

The Cas9 (CRISPR associated protein 9) system purchased from GENE company was used to delete LSD1. MGC-803 and AGS cells were transfected with lentivirus, and selected with 1.5 mg/mL puromycin for 2 days. Cells were then transferred into fresh medium without puromycin and seeded at super-low density to allow colony formation from single cells. Colonies were then picked and expanded for KO validation by western blotting. The LSD1 KO sgRNA sequence was: CCGGCCCTA CTGTCGTGCCT.

2.3. Plasmid transfection

The LSD1 overexpression plasmid was obtained from Qingke Biotechnology (Beijing, China). All transfections were performed using the Lipofectamine 2000 reagent (11668027, Life Tecghnologies, USA) according to the manufacturer's protocol.

2.4. Wound healing assay

After cells were seeded in six-well plates in culture medium, and grown to 80 % confluence, they were subjected to PBS (phosphate buffered saline) washing and wound creation with a 10 μL tip, following with indicated treatment in medium supplemented with 1% FBS. After 36 h incubation, the wound were imaged by a microscope (Nikon Ts2, Nikon, Japan).

2.5. Migration assay

Cells (8×10^3) were seeded into upper chambers with indicated treatment. The chambers were then inserted into transwell apparatus (3422, Corning, USA). Medium with 20 % FBS was added to the lower chamber. After 36 h, cells on the inserts were fixed with 4% paraformaldehyde, and then cells on the upper surface were removed by cotton swab. Cells on the bottom of the inserts were stained with DAPI (BS130A, Biosharp, China). Then cells that invaded into the lower surface were imaged and counted by High Content Screening (Thermo Fisher, USA).

2.6. Oligonucleotide transfection

Oligonucleotide, including siRNA, miR-142−5p mimic, FAM-miR-142−5p and miR-142−5p inhibitor, were used to transfect cell with Lipofectamine RNAiMax (13778, Thermo Fisher, USA) according to the manufacturer's instructions. In simple terms, cells seeded in six-well plates were transfected with an oligonucleotide at a 40 nM concentration in the presence of the Lipofectamine RNAiMax. After 6 h, medium were changed to normal standard culture medium. 24−48 h later, cells were harvested for further experiment.

miR-142−5p mimic: 5′- CAUAAAGUAGAAAGCACUACU - 3'
miR-142−5p inhibitor: 5′- AGUAGUGCUUUCUACUUUAUG - 3'
CD9 siRNA#1: 5′- AAUUGCCGUGGUCAUGAUATT - 3'
CD9 siRNA#2: 5′- GAGCAUCUUCGAGCAAGAATT - 3'

2.7. RNA extraction and quantitative real-time polymerase chain reaction

MiRNA was extracted and purified using a U6 snRNA real-time PCR Normalization Kit (Gene Pharma, China). U6 and cel-miR-39 were used as internal control and external reference control, respectively.

The following primers were used for PCR detection:
For has-mir-142−5p, F primer: AGCTCGCGCATAAAGTAGAAAG
R primer:TATGGTTGTTCTCGTCTCTGTGTC
For U6, F primer: CAGCACATATACTAAAATTGGAACG
R primer:ACGAATTTGCGTGTCATCC
For Cel-miR-39, F primer: ATATCATCTCACCGGGTGTAAATC
R primer:TATGGTTTTGACGACTGTGTGAT

2.8. Western blotting

Whole cell lysates were extracted using RIPA (radio immunoprecipitation assay) and quantified using BCA (Bicinchoninic Acid) method. After mixed with loading buffer, the sample was denatured and approximately 30 μg of protein was loaded on 10 % SDS-PAGE gel and transferred to 0.2 μm nitrocellulose membrane (P/N66485, Pall, USA). The membranes were then blocked with 5% milk in PBS for 2 h and subjected to primary antibody incubation at 4 ˚C overnight, followed by incubation with a secondary antibody conjugated with horseradish peroxidase. Finally, the blot was visualized by enhanced chemiluminescence kit (34577, Thermo Fisher, USA).

2.9. Dual luciferase reporter assay

Dual luciferase reporter assay was performed according to the manufacturer's protocol. HEK293 T cells were seeded in 96-well plate at 70–80 % confluence and incubated overnight in a 5% CO_2 incubator at 37℃. Cells were transfected with the GP-pmirGLO-CD9 3'-UTR seed region wild type, GP-pmirGLO-CD9 3'-UTR seed region mutation and GP-pmirGLO vectors with lipofectamine 2000 (11668027, Life Tecghnologies, USA), respectively, in the presence of miR-142−5p mimics. After 24 h, renilla and firefly luciferase activities were quantified using the Dual Luciferase Reporter Assay System (E1910, Promega, USA) according to the manufacturer's protocols.

The inserted CD9 3'-UTR seed region wild type sequence is: GTAT

TCATTCTGCATTGCTAGATAAAAGCTGAAGTTACTTTATGTTTGTCTTT TAATGCTTCATTCAATA;

The inserted CD9 3'-UTR seed region mutation sequence is: GTAT TCATTCTGCATTGCTAGATAAAACGAGAAGTTTGAAATAGTTTGTCTT TTAATGCTTCATTCAATA;

2.10. sEVs isolation

Cells were cultured with serum-free medium for 36 h. Then the medium was collected and centrifuged at 1500 *g* for 30 min to remove cell debris and 10,000 *g* for 30 min to remove large vesicles. After 100,000 *g* centrifugation for 2 h, the supernatant was removed, and the pellet was resuspended in 1.5 mL of PBS. The resulting pellet was washed in PBS by ultracentrifugation at 100,000 *g* for 2 h. And then the pellet was dissolved in 200 μL PBS and stored at −80 ˚C until use.

2.11. Immunofluorescence

Cells were cultured in 24-well plate. After treatment, cells were fixed with 4% paraformaldehyde and permeabilized with 0.01 % Triton X-100 for 20 min. Then cells were treated with antibodies against TSG101 (ab83, abcam, England). After washing with PBS at room temperature, cells were incubated with secondary goat anti-mouse IgG (A32727, Life, USA) for 2 h at room temperature. In addition, all samples were treated with DAPI (BS130A, Biosharp, China) for nuclues staining, and a Nikon C2 Plus confocal microscope (Nikon, Japan) was used for imaging.

2.12. MiRNA ISH (in situ hybridization)

The miRNA-ISH was carried out with miRNA ISH detection kit (G3017, Servicebio, China). Specimens were fixed in 10 % formalin solution and embedded in paraffin wax. 4 μm serial sections were cut from the tissue blocks, deparaffinized in xylene, and hydrated in a series of alcohol (75 %, 85 %, 95 %, 100 %). The tissues were digested with Proteinase K, and blocked with hydrogen peroxide and pre-hybridization solution. Then, digoxigenin labeled locked nucleic acid probes antisense to miR-142−5p were hybridized on tissue sections for one night at 37 ℃, and followed by incubating with anti-DIG-HRP for 30 min. at 37 ℃. Finally, the section was stained with DAB kit (ZL1−9018, ZSGB-BIO, China), the nucleus was stained with hematoxylin. After staining, the sections were digitally scanned using the Aperio AT2 scanner (Leica Biosystems, Germany), and analyzed with Aperio image Analysis workstation (Leica Biosystems, Germany).

2.13. Tissue specimens and IHC (immunohistochemistry)

Specimens were fixed in 10 % formalin solution and embedded in paraffin wax. 4 μm serial sections were cut from the tissue blocks, deparaffinized in xylene, and hydrated in a series of alcohol (75 %, 85 %, 95 %, 100 %), followed by antigen retrieval with EDTA. Tissue sections were then incubated with primary antibodies (LSD1, ab129195, abcam, UK; CD9, 134403, CST, USA; Dicer, 5362 T, CST, USA; AGO2, 2897 T, CST, USA). Subsequently, tissue sections were incubated with secondary antibody (Peroxidase-conjugated goat anti-rabbit Ig, ZB-2301, Zsbio, China; peroxidase-conjugated goat anti-mouse IgG, ZB-2305, Zsbio, China) for 2 h at room temperature, and then stained with DAB kit (ZL1−9018, ZSGB-BIO, China). After staining, sections were digitally scanned using the Aperio AT2 scanner (Leica Biosystems, Germany), and analyzed with Aperio image Analysis workstation (Leica Biosystems, Germany) using a pathologist-trained nuclear, cytoplasmic, nuclear & cytoplasmic, and cytoplasmic - specific algorithm, respectively. Protein expression was evaluated according to the H-Score obtained from Aperio image Analysis workstation.

2.14. Ethics declarations

Gastric cancer tissues and adjacent tissues were obtained from the First Affiliated Hospital of Zhengzhou University and Henan Cancer Hospital Affiliated to Zhengzhou University. All human tissues were collected using protocols approved by the Ethics Committee of the Zhengzhou University Health Science Center.

2.15. Lung metastasis model

Five weeks old female BALB/c nude mice were purchased from Jingda Laboratory Animal, Hunan, China. All animals were housed in a pathogen-free environment, and experimental protocols were approved by the Ethics Committee of the Zhengzhou University Health Science Center. To evaluate metastasis, 1×10^6/100 μL cells were injected into nude mice through tail vein. 28 days later, the mice were euthanized, and lung of mice was collected and subjected to metastatic nodules counting.

2.16. Intracardiac injection metastatic model

For intracardiac injection model, luciferase labeled cells were injected into the left ventricle (2.5×10^5 cells) of 6-week-old female NOD/SCID mice that were purchased from Jingda Laboratory Animal, Hunan, China. For bioluminescence imaging, mice were anesthetized using isoflurane and given 150 mg/g of D-luciferin in PBS by i.p. injection, bioluminescence was determined with IVIS Spectrum (PerkinElmer, USA). Bioluminescence images were obtained with a 15 cm field of view, and an imaging time of 30 s to 2 min. Bioluminescence from relative optical intensity was defined manually, and data were expressed as photon flux and were normalized to background photon flux, which was defined from a relative optical intensity drawn over a mouse that was not given an injection of luciferin. After the bioluminescence imaging at the sixth week, we continued to raise mice for another 3 weeks to obtain their survival curve. All animals were housed in a pathogen-free environment, and experimental protocols were approved by the Ethics Committee of the Zhengzhou University Health Science Center.

2.17. Statistical analysis

Pearson correlation coefficient was used to evaluate the correlationship between groups. Results were considered statistically significant at $P < 0.05$. $P < 0.01$ was considered highly significant. All analysis was carried out using SPSS 21.0 software. In this study, the statistical analyses were performed with Student's *t* Test. $^*P < 0.05$, $^{**}P < 0.01$, $^{**}P < 0.001$.

3. Results

3.1. Inhibition of LSD1 attenuates gastric cancer cell migration

LSD1 was reported as an oncogene in multiple cancers [5–7], although its oncogenicity has not been clarified in GC. To reveal the biological role of LSD1 in GC, expression analysis with GEPIA (http://gepia.cancer-pku.cn/) was performed firstly [24], and the data showed that LSD1 was highly expressed in GC tissues compared to normal tissues (Fig. 1A). Then, to further assess LSD1 on survival outcome in GC patient, meta-analysis was carried out on Kaplan-Meier Plotter (http://kmplot.com/analysis/) [25], and result showed that GC patients with high level of LSD1 performed poor survival outcome (Fig. 1B). These data suggested the potential oncogenicity of LSD1 in GC.

To validate whether LSD1 plays as a promoter in GC development, 522 paired GC patient tissues were collected, and the clinicopathological data were summarized and described in Table S1. Statistics showed that the incidence of GC in men was almost three

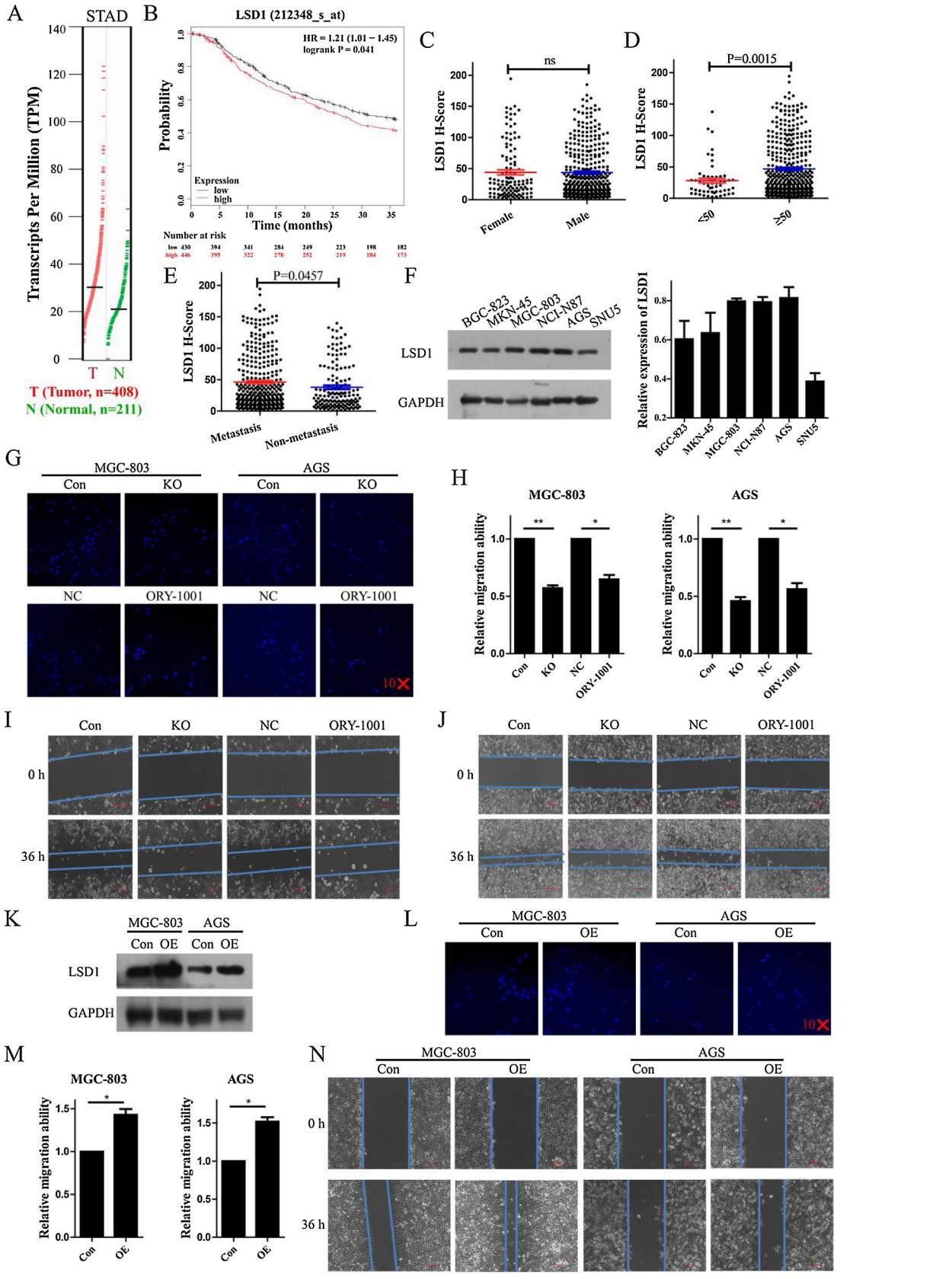

(caption on next page)

Fig. 1. Inhibition of LSD1 attenuates gastric cancer cell migration. A, mRNA level of LSD1 in GC tissues or normal tissues analyzed with GEPIA; B, Overall survival analysis using Kaplan-Meier Plotter with LSD1 as an index; C–F, LSD1 expression in different groups with diverse clinical factors as indexes (C, gender; D, age; E, metastasis); F, Expression of LSD1 in BGC-823, MKN-45, MGC-803, NCI-N87, AGS and SNU5 cell lines; G & H, Transwell assay in MGC-803 and AGS cells when LSD1 was knocked out for 36 h, fluorescence images were taken (G) and quantified (H) with DAPI staining coupled with high content screening; I & J, Wound healing assay with indicated treatment in MGC-803 (I) and AGS (J) cells, Con and NC represents the negative control for LSD1 KO and ORY-1001, bar = 200 μm; K, Expression of LSD1 in MGC-803 and AGS cell lines when LSD1 was overexpressed; L & M, Transwell assay in MGC-803 and AGS cells when LSD1 was overexpressed 36 h, fluorescence images were taken (L) and quantified (M) with DAPI staining coupled with high content screening; N, Wound healing assay when LSD1 was overexpressed in MGC-803 and AGS cells. ns: no significant difference, * $P < 0.05$, ** $P < 0.01$.

times of that in women, and most GC patients (88.31 %) were older than 50 years old. Moreover, 70.31 % of patients with GC were accompanied with lymphatic metastasis, and only a small part of patients (2.68 %) was in well differentiated stage. Thus, it was a pervasive and malign phenomenon that the diagnosed GC patients were always accompanied with metastasis and poor differentiation, indicating their poor outcome in clinic.

To further clarify the role of LSD1 in GC, IHC staining of LSD1 was performed (Figure S1A) and analyzed in corresponding to diverse clinical factors. Result showed that there was no significant difference on the expression of LSD1 between genders (Fig. 1C), while the expression of LSD1 was significantly higher in elder patients (more than 50 years old) and patients with metastasis (Fig. 1D and E). Overall, these data prompted us to hypothesize that LSD1 may be involved in the development of GC, especially in GC metastasis.

Although we have reported that LSD1 inhibitors could suppress GC cells metastasis previously [26], how does LSD1 promote GC metastasis is still unclear. Before the following study to answer this question, expression of LSD1 in diverse GC cells was scanned, and MGC-803 and AGS were selected for following studies due to their rich content of LSD1 (Fig. 1F). To further characterize LSD1 as a migration promoter in GC, MGC-803 LSD1 KO and AGS LSD1 KO cell lines were established (Figure S1B) and subjected to transwell experiment. As illustrated in Fig. 1G & H, both LSD1 KO and LSD1 inhibitor (ORY-1001) considerably attenuated the migration ability of MGC-803 and AGS cells. Besides, wound healing assay was performed to further verify the contribution of LSD1 to GC cells migration. Results in Fig. 1I & J indicated that the migration of cancer cells was significantly reduced in LSD1 KO cells or ORY-1001 treated cells. To further verify the positive role of LSD1 in gastric cancer migration, we overexpressed LSD1 in MGC-803 and AGS cells (Fig. 1K). As shown in Fig. 1L-N, overexpressed LSD1 could considerably enhance the migration ability of MGC-803 and AGS cells. All these results indicate the positive role of LSD1 in GC cell migration. However, the mechanism about LSD1 in GC cell migration remains largely unknown.

3.2. LSD1 is the upstream regulator of miR-142−5p

MiRNAs are small endogenous RNAs that regulate gene-expression post-transcriptionally. It has been an exciting area of research for their roles in multiple diseases [27]. In 2018, Yang Shi et al. found that loss of LSD1 can lead to dsRNA accumulation by down regulating the expression of RISC components and consequently RISC function [14], which couples with miRNA biogenesis also. This message prompted us to explore if LSD1 accelerates GC cells migration with the aid of miRNA. Firstly, to clarify whether LSD1 regulates miRNA biogenesis, Dicer and AGO2 as core members of RISC components were chose to study clinically. As illustrated in Fig. 2A, LSD1 performed closely correlationship with Dicer ($R_{LSD1/Dicer} = 0.42$, $P < 0.0001$) and AGO2 ($R_{LSD1/AGO2} = 0.45$, $P < 0.0001$) in GC with data from GEPIA (http://gepia.cancer-pku.cn/) [24]. To further verify the relationship between LSD1 and Dicer (Figure S2A), our in-house GC patient tissue library was applied for IHC staining. Result in Fig. 2B displayed that LSD1 performed a positive correlationship with Dicer ($R = 0.2852$, $P = 0.0103$) in 80 LSD1 overexpressed GC tissues with lymphatic metastasis, although LSD1 performed a negative correlationship with Dicer in tissues without classification ($R = -0.3411$, $P < 0.0001$; Fig. 2C). The above results further verify the potential of LSD1 in miRNA biogenesis in GC patient with metastasis.

Based on the analysis above, we concluded the potential of LSD1 in GC metastasis and miRNA biogenesis, but the detailed mechanism is still in vague and needs to be clarified, and we supposed that LSD1 may accelerate GC metastasis by regulating metastasis related miRNA. With preliminary research, we found miR-142−5p was reported to be a potential marker in clinic on metastatic melanoma and non-small cell lung cancer [28–30]. Then, the overview expression of miR-142−5p in cancer tissues and normal tissues was searched on GEDS (http://bioinfo.life.hust.edu.cn/web/GEDS/) [31]. As depicted in Table 1, miR-142−5p was overexpressed in many types of cancer, including GC. Following this finding, the correlation of miR-142−5p on GC patient prognosis was analyzed on ONCOMIR (http://www.oncomir.org/) [32]. As depicted in Fig. 2D, the overall survival rate of low miR-142−5p expression patient was significantly higher than patients with high miR-142−5p expression ($P < 0.0001$). Besides, miR-142−5p was revealed to be an accelerator of renal cell carcinoma migration [33]. These findings of miR-142−5p in cancer metastasis and GC prognosis are consistent with LSD1, which prompted us to speculate that miR-142−5p may be the potential miRNA affected by LSD1 and involved in the regulation of LSD1 on GC metastasis. Consequently, miRNA ISH assay was performed to verify the expression level of miR-142−5p in GC (Figure S2B), and miR-142−5p was confirmed to be overexpressed in GC tissues (Fig. 2E) and also metastatic GC tissues (Figure S2C). Further correlation analysis revealed that there was a significant correlation between LSD1 and miR-142−5p ($R = 0.4102$, $P < 0.0001$; Fig. 2F). Additionally, LSD1 displayed a closer relationship with miR-142−5p in tissues with metastasis ($R = 0.4332$, $P < 0.0001$; Fig. 2G) than in tissues with non-metastasis ($R = 0.3035$, $P = 0.0013$; Fig. 2H). These results indicated that miR-142−5p performed a close relationship with both GC metastasis and LSD1, which further drove us to verify the regulation of LSD1 on miR-142−5p. Therefore, expression levels of Dicer and AGO2 in MGC-803 and AGS cell lines were detected, and decreased levels of Dicer, AGO2 (Fig. 2I) as well as miR-142−5p (Fig. 2J) were observed in MGC-803 and AGS cells when LSD1 was absent. All these results together suggest that absence of LSD1 may blunt the expression of Dicer and AGO2, and cause the decreasing of miR-142−5p as an upstream regulator.

3.3. MiR-142−5p promotes GC cell migration via targeting CD9

The above results indicated that absence of LSD1 may decrease the intracellular miR-142−5p by blunting the expression of Dicer and AGO2. But role of miR-142−5p in GC metastasis is still indeterminate. As shown in Fig. 3A, treatment of MGC-803 and AGS cells with miR-142−5p mimic caused stronger migration capacity, while inhibitor of miR-142−5p suppressed the migration capacity of treated cells. Nevertheless, how does miR-142−5p promote cell migration remains unknown. To answer this question, target of miR-142−5p was searched with the TargetScan [34] and miRBase [35] databases, and CD9, which is associated with cell migration, was identified as a potential target for miR-142−5p (Fig. 3B). To further characterize CD9 as the target of miR-142−5p, miR-142−5p mimic and inhibitor were transfected into MGC-803 and AGS cell lines. As suggested in Fig. 3C, mimic addition

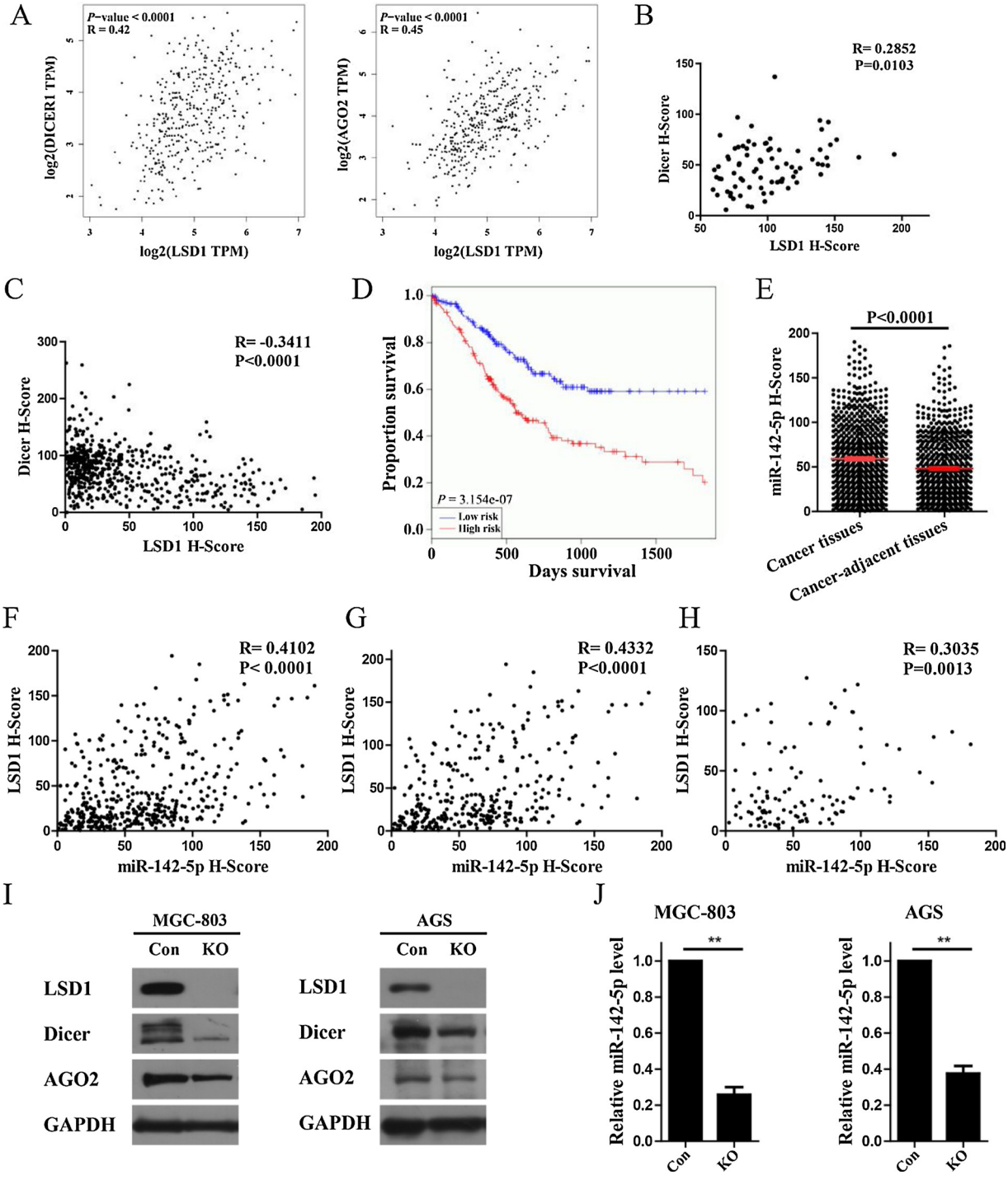

Fig. 2. LSD1 may positively regulate the biogenesis of miR-145-5p. A, Correlationship between LSD1 and Dicer & AGO2 in mRNA level with data analyzed on GEPIA (http://gepia.cancer-pku.cn/); B, Correlationship between LSD1 and Dicer in 80 LSD1 overexpressed GC tissues with lymphatic metastasis; C, Correlationship between LSD1 and Dicer in GC tissues without classification; D, Patient prognosis with miR-142-5p as an index was analyzed with ONCOMIR (http://www.oncomir.org/); E, Expression of miR-142-5p in 522 GC tissues and cancer-adjacent tissues; F - H, Correlationship between LSD1 and miR-142-5p in unclassified GC tissues (F), 367 GC tissues with lymphatic metastasis (G), and 155 GC tissues without lymphatic metastasis (H); I, Expression of LSD1, Dicer and AGO2 when LSD1 was knocked out in MGC-803 and AGS cells, respectively, GAPDH was used as loading control; J, Quantification of miR-142-5p when LSD1 was knocked out in MGC-803 and AGS cells, respectively. **P < 0.01.

markedly attenuated the expression of CD9, while inhibitor addition led to an increase of CD9, which characterized CD9 as the downstream target of miR-142 − 5p. But whether miR-142 − 5p binds to CD9 directly as a suppressor is still unclear. The information on TargetScan gave the prediction that miR-142 − 5p may bind to the 151–157 position of 3'-UTR region of CD9. To validate this speculation, dual luciferase reporter system was applied with 3'-UTR-WT or 3'-UTR-Mut of CD9 to validate the direct interaction between miR-142 − 5p and CD9 in the presence of miR-142 − 5p mimic. Result in Fig. 3D indicated that miR-142 − 5p mimic can significantly decrease the luciferase activity in cells transfected with 3'-UTR-WT of CD9, but not 3'-UTR-Mut of CD9. Hence, with the data above, we confirmed that CD9 is a new target of miR-

Table 1
Amount of miR-142-5p in different cancers and corresponding normal tissues analyzed by ONCOMIR website (http://www.oncomir.org/).

miRNA Name	Cancer	*t* -test P-value	*t* -test FDR	Upregulated	Tumor Log2(Mean Expression)	Normal Log2 (Mean Expression)
hsa-miR-142 – 5p	BLCA	4.52e-02	9.24e-02	Tumor	5.54	4.38
hsa-miR-142 – 5p	BRCA	9.10e-10	4.05e-09	Tumor	5.69	4.55
hsa-miR-142 – 5p	CESC	3.14e-02	3.02e-01	Tumor	6.09	2.60
hsa-miR-142 – 5p	COAD	4.50e-05	3.45e-04	Tumor	6.07	0.28
hsa-miR-142 – 5p	ESCA	3.51e-03	2.16e-02	Tumor	5.68	4.21
hsa-miR-142 – 5p	KIRC	3.77e-16	3.07e-15	Tumor	5.79	3.66
hsa-miR-142 – 5p	KIRP	6.55e-03	1.49e-02	Tumor	5.08	4.13
hsa-miR-142 – 5p	LIHC	1.24e-09	1.68e-08	Normal	5.22	6.84
hsa-miR-142 – 5p	LUAD	4.71e-03	1.56e-02	Tumor	6.55	5.30
hsa-miR-142 – 5p	PAAD	4.95e-02	4.42e-01	Normal	4.80	7.57
hsa-miR-142 – 5p	PRAD	1.15e-05	5.28e-05	Tumor	4.42	3.63
hsa-miR-142 – 5p	READ	3.13e-03	3.42e-02	Tumor	7.04	0.15
hsa-miR-142 – 5p	STAD	2.22e-05	9.14e-05	Tumor	6.61	4.77
hsa-miR-142 – 5p	THCA	7.06e-06	2.69e-05	Normal	5.04	5.96
hsa-miR-142 – 5p	UCEC	4.19e-04	1.31e-03	Tumor	4.98	3.30

BLCA: bladder urothelial carcinoma; **BRCA**: breast invasive carcinoma; **CESC**: cervical squamous cell carcinoma and endocervical adenocarcinoma; **COAD**: colon adenocarcinoma; **ESCA**: esophageal carcinoma; KIRC: kidney renal clear cell carcinoma; **KIRP**: kidney renal papillary cell carcinoma; **LIHC**: liver hepatocellular carcinoma; **LUAD**: lung adenocarcinoma; **PAAD**: pancreatic adenocarcinoma; **PRAD**: prostate adenocarcinoma; **READ**: rectal adenocarcinoma; **STAD**: stomach adenocarcinoma; **THCA**: thyroid carcinoma; **UCEC**: uterine corpus endometrial carcinoma.

142 – 5p, and miR-142 – 5p may bind to the 3'-UTR of CD9 to suppress its translation.

Aberrant loss of CD9 has been implicated as a key obstruction of cell migration in many types of cancer [36–39], including GC [40]. To further verify the role of CD9 in GC metastasis again here, the influence of CD9 on GC patient prognosis was analyzed firstly with Kaplan-Meier Plotter (http://kmplot.com/analysis/) [25]. As depicted in Fig. 3E, the overall survival rate of high CD9 expression patient was significantly better than patients with low CD9 expression (HR = 0.72, P = 0.00013). Additional wound healing assay (Fig. 3F &G) and transwell assay (Fig. 3H) confirmed that CD9-siRNA treatment could promote the migration ability of MGC-803 and AGS cells, while LSD1 was kept constant in the absent of CD9 (Figure S3A). All these results indicate that CD9 was not the upstream regulator of LSD1 and miR-142 – 5p promotes GC cell migration by targeting CD9, a novel substrate of miR-142 – 5p.

3.4. LSD1 negatively regulates CD9 and promotes GC cells migration mediated by miR-142 – 5p

The above results have proved that miR-142 – 5p participates in the regulation of LSD1 on GC cell migration, and LSD1 is the upstream regulator of miR-142 – 5p. Meanwhile, miR-142 – 5p promotes GC cell migration *via* targeting CD9. But whether LSD1 could regulate CD9 *via* miR-142 – 5p remained to be explored. So, we supposed that miR-142 – 5p may form a bridge between LSD1 and CD9. To validate our hypothesis, IHC was performed, and CD9 was highly expressed in non-metastatic GC tissues (Figure S3B & C). Besides, correlation analysis in Fig. 4A revealed that there was a significant negative correlation between LSD1 and CD9 in GC tissues with lymphatic metastasis (R = -0.4689, P < 0.0001). Consistent with this negative correlation between LSD1 and CD9, increased level of CD9 was observed in LSD1 abrogated MGC-803 and AGS cells (Fig. 4B). Moreover, LSD1 absent induced CD9 upregulation can be attenuated by miR-142 – 5p mimic (Fig. 4C). At the same time, overexpression of miR-142 – 5p could rescue the decreased migration ability of gastric cancer cells caused by LSD1 deletion (Fig. 4D & E). These results indicate that LSD1 deletion can up-regulate CD9 *via* reducing intracellular miR-142 – 5p, which is a novel way for LSD1 to accelerate GC migration.

3.5. Secretion of miR-142 – 5p into sEVs contributes to decreased intracellular miR-142 – 5p

As LSD1 abrogation can reduce the level of miR-142 – 5p, but is there another way to decrease intracellular miR-142 – 5p besides blocking miRNA biogenesis? So, we turned our attention to the release of miR-142 – 5p outside the cell. We have shown that LSD1 could regulate CD9, a protein marker of sEVs, *via* miR-142 – 5p, and sEVs can deliver nucleic acids, proteins or lipids out of cells [39,41–43]. Therefore, we speculated that LSD1 could also regulate miR-142 – 5p by sEVs. To determine whether miR-142 – 5p was affected by sEVs when LSD1 was abrogated, sEVs were isolated using ultracentrifuge method and the transmission electron microscopy displayed typical cup-shaped morphology of sEVs (Fig. 5A). Additional NTA measurements also showed that the size of isolated particles was range from 40 to 150 nm, which was within the expected size range for sEVs (Fig. 5B & C). The detection of sEVs positive marker proteins CD9 and Alix and the negative protein marker calnexin further confirmed the successful isolation of sEVs (Fig. 5D). Then the following analysis showed that the amount of miR-142 – 5p was higher in sEVs isolated from LSD1 KO cells than that in parent cells in both MGC-803 and AGS cells (Fig. 5E). To gain insight into how does LSD1 abrogation promote the secretion of miR-142 – 5p into sEVs, co-localization of miR-142 – 5p with TSG101, a marker of MVBs (multivesicular bodies), was investigated [44,45] as MVBs are late endosomes containing cargo and the cargo can be released extracellularly as sEVs [46]. Results in Fig. 5F-I revealed that LSD1 abrogation lead to increased amount of TSG101 and there was less miR-142 – 5p colocalized with TSG101 in LSD1 abrogated MGC-803 (Fig. 5F & G) and AGS (Fig. 5H & I) cells than the control groups. These results suggested that LSD1 abrogation promoted the generation of MVBs loaded with miR-142 – 5p, which can be secreted extracellularly, resulting in decreased amount of miR-142 – 5p intracellularly. To further validate LSD1 could export miR-142 – 5p by sEVs, we treated the LSD1 KO cells with GW4869, the sEVs secretion inhibitor [47]. As shown in Fig. 5J, LSD1 deletion could decrease miR-142 – 5p intracellularly, but GW4869 could partially rescue the decrease of miR-142 – 5p caused by LSD1 deletion in MGC-803 cells and AGS cells. All these findings further verify that promoting the secretion of miR-142 – 5p using sEVs vehicles is another way for LSD1 abrogation to down-regulate intracellular miR-142 – 5p.

3.6. LSD1 KO attenuates GC metastasis by up-regulating CD9 via decreasing intracellular miR-142 – 5p in vivo

To further confirm the role of miR-142 – 5p in LSD1 mediated metastasis of GC cells *in vivo*, lung metastasis model was applied with MGC-803 and MGC-803 LSD1 KO cells. 4 weeks after the tail injection, mice were sacrificed and lungs were stripped and subjected to HE

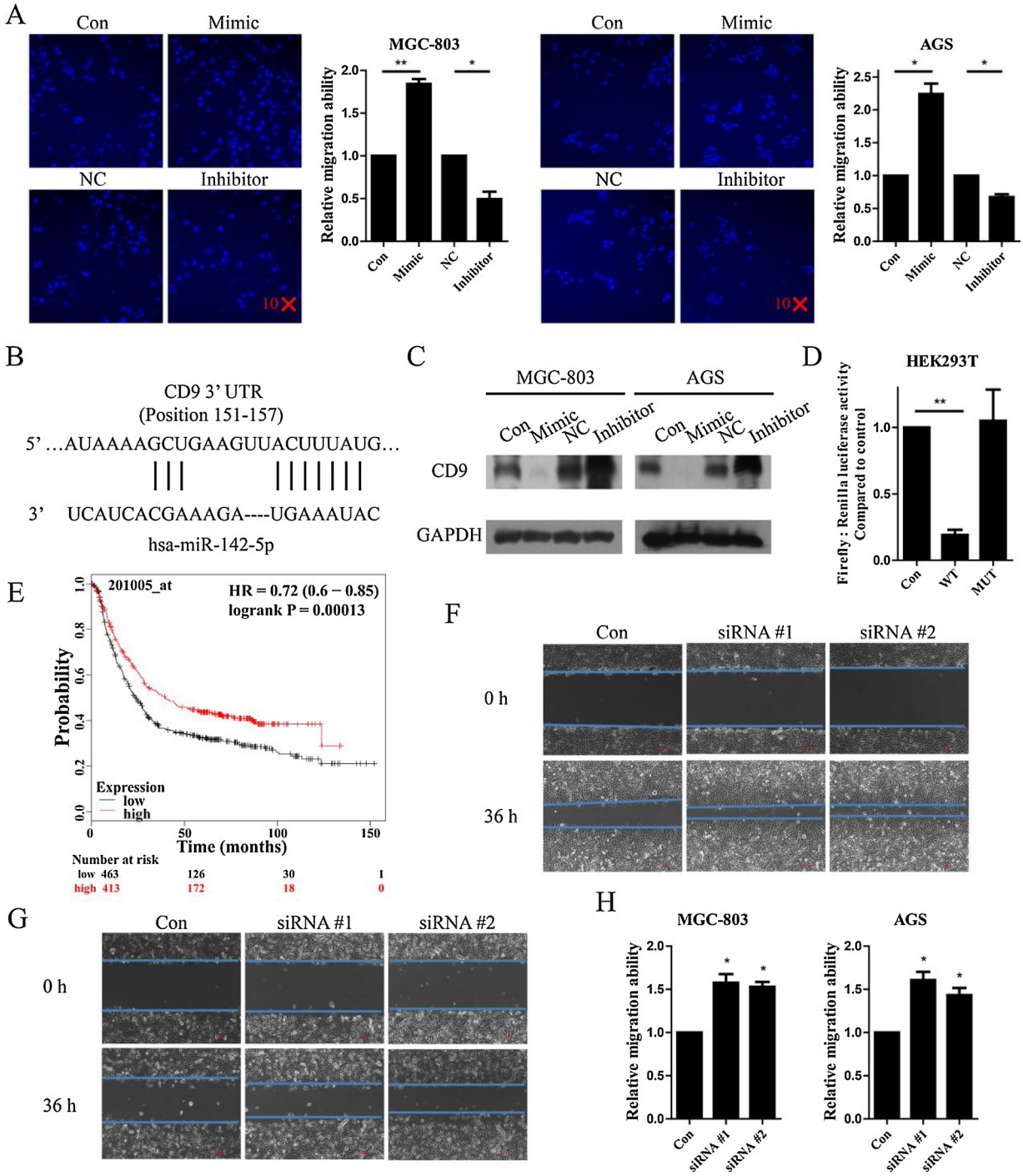

Fig. 3. LSD1 KO attenuates GC migration by down-regulating intercellular miR-142-5p to up-regulate CD9. A, Transwell assay was performed in MGC-803 and AGS cells with indicated treatment, the migrated cells were imaged and quantified with high content screening; B, Sequence alignment between CD9 3'-UTR and miR-142-5p; C, Expression of CD9 in MGC-803 and AGS cells with additional miR-142-5p mimic and miR-142-5p inhibitor, respectively; D, Dual luciferase reporter assay of miRNA-142-5p on 3'-UTR-WT and 3'-UTR-Mut of CD9 in HEK293 T cells; E, Patient prognosis with CD9 as an index analyzed on Kaplan-Meier Plotter (http://kmplot.com/analysis/); F & G, Wound healing assay in MGC-803 (F) and AGC (G) cells transfected with CD9-siRNAs, bar = 100 μm; H, Transwell assay in MGC-803 and AGC cells transfected with CD9-siRNAs. * $P < 0.05$, ** $P < 0.01$.

(hematoxylin-eosin) staining, and results confirmed the lung metastasis in control group was stronger than that in LSD1 KO group (Fig. 6A & B). Subsequently, expression of LSD1, CD9 and miR-142−5p in the metastatic nodules of the control group and the LSD1 KO group were detected, and results showed that with the disappearance of LSD1, amount of miR-142−5p was decreased, while the expression of CD9 was increased significantly (Fig. 6C), which was consistent with *in vitro* studies. Meanwhile, the control group showed a trend of weight loss in the later period of the experiment, although it was not so significant (Fig. 6D).

Besides, intracardiac injection model was also applied to NOD-SCID mice using luciferase labeled MGC-803 and MGC-803 LSD1 KO cells. During the feeding time, the mice were imaged and quantified using bioluminescence imaging, and Fig. 6E indicated that the metastasis of cancer cells was significantly reduced in mice injected with LSD1 KO cells. Survival analysis also demonstrated that, compared to the control

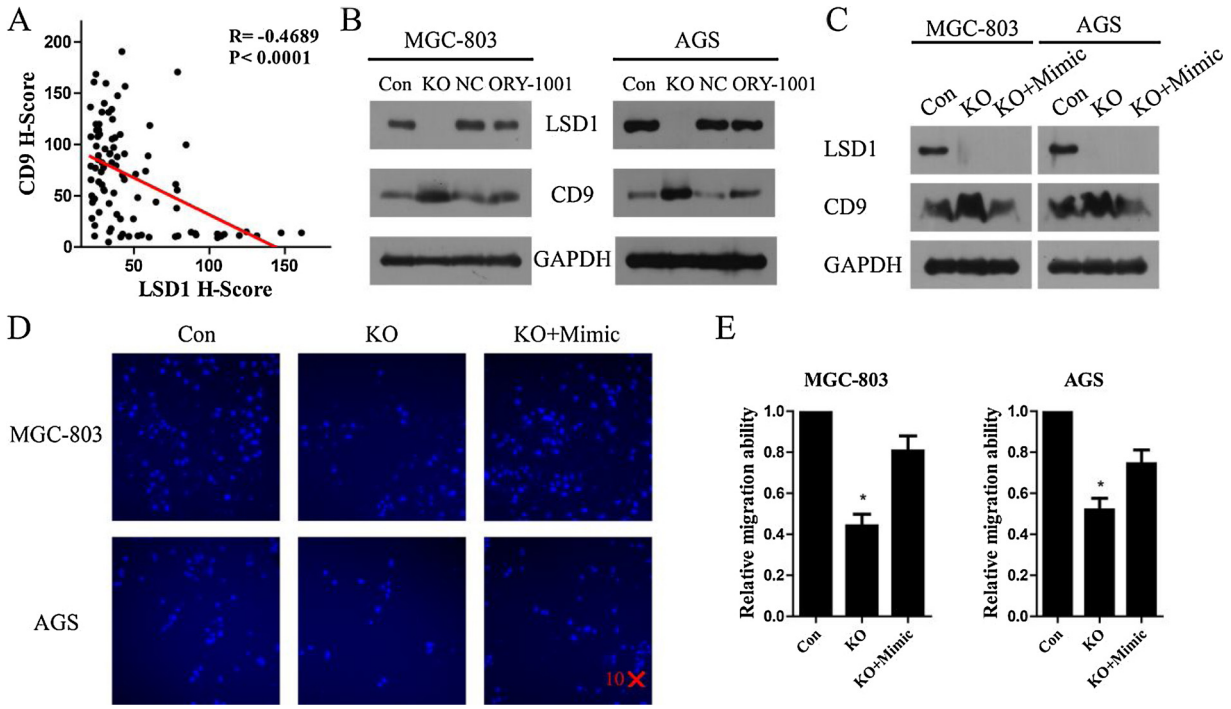

Fig. 4. LSD1-miR-142-5p axis negatively regulates CD9 and promotes GC cells migration. A, Correlationship between LSD1 and CD9 in 80 GC patients with lymphatic metastasis; B, Expression of CD9 in MGC-803 and AGS cells when LSD1 was abrogated genetically or pharmacologically, respectively; C, Expression of CD9 in MGC-803 and AGS cells when LSD1 was deleted in the presence of miR-142-5p or not; D & E, Transwell assay was performed with indicated treatment for 36 h in MGC-803 and AGS cells, respectively, fluorescence images were taken (D) and quantified with high content screening (E). * $P < 0.05$, ** $P < 0.01$.

group, the group with LSD1 KO exhibited a significantly improvement in their survival time (Fig. 6F). Similar to the lung metastasis model, the group with LSD1 KO exhibited a more stable body weight here, while control group showed a trend of losing weight, although it was not so significant (Fig. 6G). With all the above evidence, we could conclude that LSD1 KO attenuates GC metastasis by downregulating intracellular miR-142−5p to up regulate CD9 *in vivo*.

4. Discussion and conclusion

Although it is the effectively choice for cancer patients to accept surgery and chemotherapy, metastasis still occurs frequently, and it is the major cause of treatment failure and mortality in individuals [48]. As the culprit behind most cancer-related deaths, metastatic process is a complex sequence of events [49]. Thus, it is urgent to understand the mechanism of cancer metastasis occurrence and development.

LSD1 is highly expressed in several cancer cells, suggesting a widespread oncogenic role [7]. It had been reported to be involved in many cellular signaling pathways as well as the initiation and development of cancers since its identification in 2004 [50–52], and LSD1 inhibitors have also been extensively developed [53–55]. As our group found that LSD1 inhibitors could effectively inhibit the migration of gastric cancer cells [26,56], we would like to further clarify the mechanism of LSD1 in GC migration. In this study, LSD1 was found to be overexpressed in metastatic GC tissues as a contributor of GC metastasis. Due to the serious threat of gastric cancer metastasis to patient survival, coupled with the unclear mechanism of LSD1 on gastric cancer metastasis, we hoped to further understand the mechanism of LSD1 as a metastatic contributor in GC. The analysis based on TCGA and our in-house tissue library gave us an important hint that LSD1 may affect some miRNAs synthesis because of the close relationship between LSD1 and Dicer and AGO2, which both are important members in miRNA biogenesis. As a demethylase, LSD1 has the ability to remove methylation of many substrates, including histone and non-histone substrates. But its impact on miRNA is still in blank. After the screening, it is excited to find that miR-142−5p was closely related to cancer metastasis [33], and had a significant positive correlation with LSD1 in tissues with metastasis. All these results suggested that miR-142−5p may participate in the contribution of LSD1 on GC metastasis. Further experiments have verified that the absence of LSD1 reduces the intracellular level of miR-142−5p, which demonstrated that LSD1 was an upstream regulator of miR-142−5p. So, further search for target genes was performed as targeting mRNAs is the classical way for miRNA to function on gene silencing and translational repression [57] and CD9 was identified as a novel miR-142−5p downstream target. Tetraspanin CD9 was first described as a motility-related factor in 1991 [58], which was confirmed as a suppressor of cell motility and metastasis [59]. In our study, down-regulated CD9 contributed to the cell migration and poor survival outcome of GC patients (Fig. 3E-G), and abrogated LSD1 resulted in the augment of CD9, which could be reversed by addition of miR-142−5p mimic. Make a general survey of these results, miR-142−5p was proved to be a bridge between LSD1 and CD9. LSD1/miR-142−5p/CD9 axis shows a new pathway for abrogated LSD1 to inhibit GC metastasis. Moreover, the data revealed that abrogated LSD1 promoted the secretion of miR-142−5p into sEVs, which was another way for LSD1 KO to decrease intracellular miR-142−5p. This finding indicates that abrogation of LSD1 may also promote the loading of miRNA into sEVs, which will be a new direction for the biological function of LSD1.

5. Conclusions

LSD1 has been recognized as a demethylase to exert its biological effects by removing the methyl group from its substrate. But, there is hardly report on its regulation on miRNAs. This article revealed a new branch of LSD1 substrates. The further clarity mechanism of LSD1 as a GC metastasis contributor will play an important guiding role in the clinical application of LSD1 inhibitor.

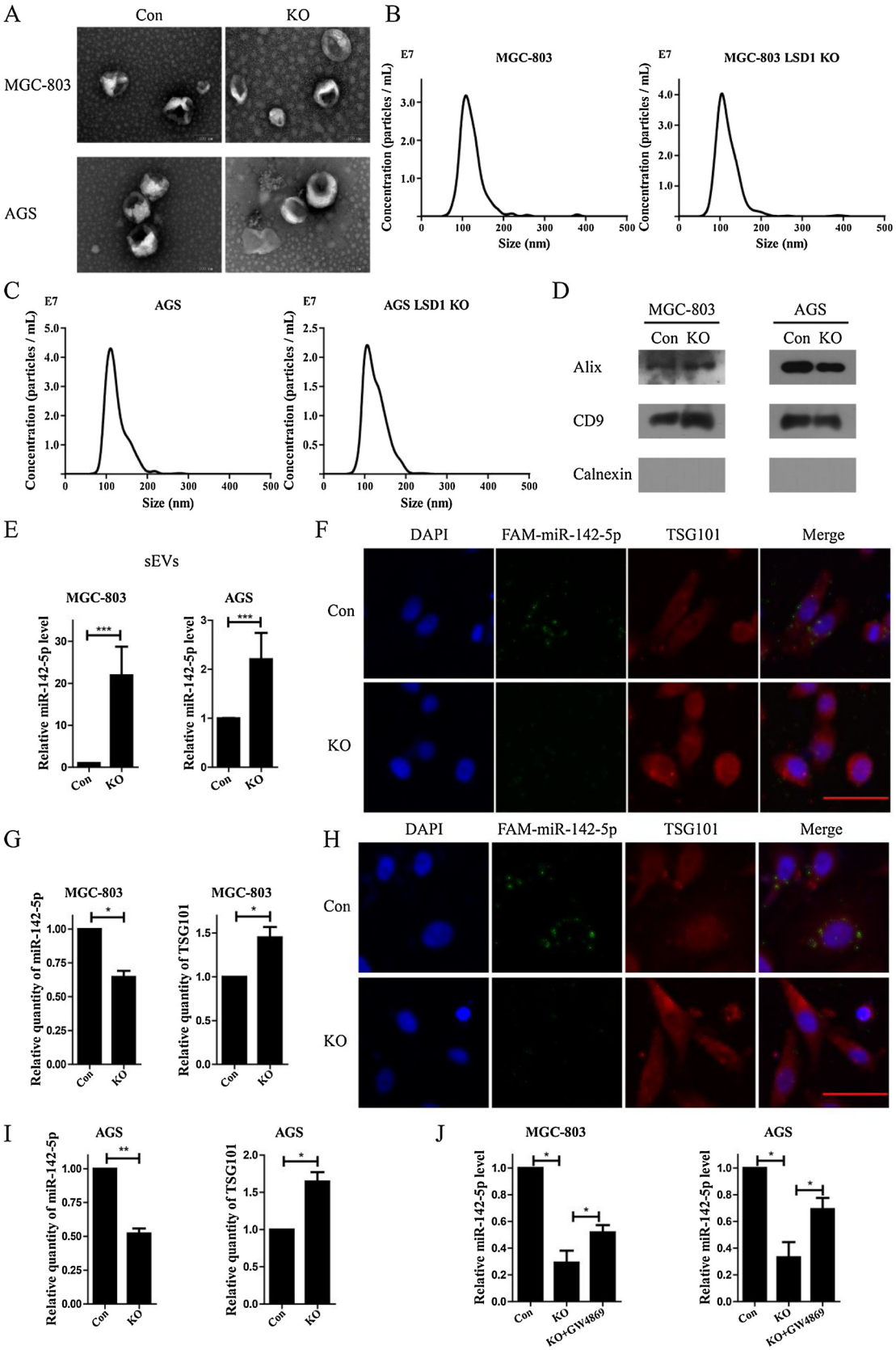

Fig. 5. Abrogated LSD1 enhances the secretion of miR-142-5p by sEVs. A, Transmission electron microscope scanning of sEVs isolated from indicated cells; B & C, Size profiles of sEVs released by MGC-803 (B) and AGS (C) cells were evaluated by NTA; D, Alix and CD9 were detected as the sEVs markers, and calnexin was used as the negative marker of sEVs; E, Amount of miR-142-5p in MGC-803 and AGS cells derived sEVs in the presence of LSD1 or not; F - I, In the presence of LSD1 or not, co-localization of TSG101 (red) and additioned FAM-miRNA-142-5p (green) were imaged (F & H) and quantified (G & I) in MGC-803 and AGS cells, bar = 25 μm; J, Amount of intracellular miR-142-5p in MGC-803 and AGS cells with indication. *P < 0.05, **P < 0.01, ***P < 0.001.

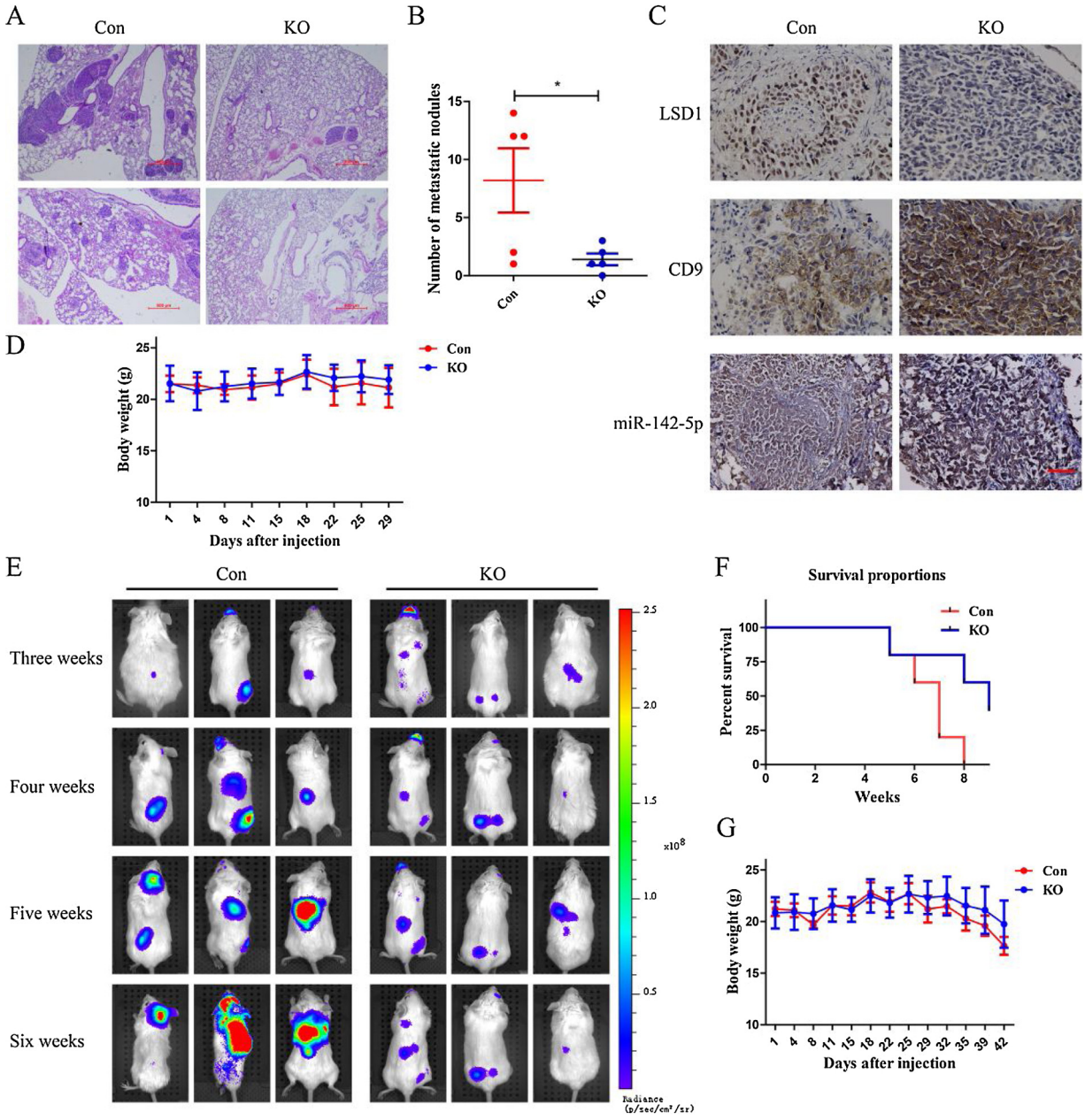

Fig. 6. LSD1 KO attenuates GC metastasis by downregulating intracellular miR-142-5p to up regulate CD9 *in vivo*. A, HE staining of lung metastasis from control or LSD1 KO groups, bar = 500 μm; B, Number of metastatic nodules in lung was counted; C, Expression of LSD1 and CD9 in metastatic nodules were detected by IHC and miR-142-5p was quantified by ISH; D, Body weight of control and LSD1 KO groups in lung metastasis modesl; E, Effect of LSD1 on seeding metastasis following intracardiac injection of MGC-803 and MGC-803 LSD1 KO cells in 6-week-old NOD-SCID mice (n = 5). Cell metastasis was quantified using bioluminescence imaging 3 weeks after injection weekly; F, Kaplan-Meier survival plot of control and LSD1 KO groups in intracardiac injection model; G, Body weight of control and LSD1 KO groups in intracardiac injection metastasis model. *P < 0.05.

Author contributions

Li-Juan Zhao wrote the manuscript. Li-Juan Zhao, Qi-Qi Fan and Ying-Ying Li performed the experiment. Li-Juan Zhao contributed to the IHC and evaluated the results with Hong-Mei Ren. Li-Juan Zhao, Ting Zhang, Shuan Liu and Mamun Maa contributed to the *in vivo* experiment. Yi-Chao Zheng contributed to critical revision of the manuscript. Hong-Min Liu and Yi-Chao Zheng designed the study and finalized the manuscript.

Declaration of Competing Interest

The work described has not been submitted elsewhere for publication, in whole or in part, and all the authors listed have approved the manuscript that is enclosed. The authors declare that they have no competing interests.

Acknowledgements

This work was supported by National Natural Science Foundation of China (Nos. 81602961, 81430085 and 21372206); National Key Research Program (Nos. 2018YFE0195100, 2016YFA0501800 and 2017YFD0501401); Science and Technology Innovation Talents of Henan Provincial Education Department (19IRTSTHN001); Basic and Frontier Technology Research Project of Henan Province (No. 162300410119).

Appendix A. Supplementary data

Supplementary material related to this article can be found, in the online version, at doi:https://doi.org/10.1016/j.phrs.2020.104991.

References

[1] F. Bray, J. Ferlay, I. Soerjomataram, R.L. Siegel, L.A. Torre, A. Jemal, Global cancer statistics 2018: GLOBOCAN estimates of incidence and mortality worldwide for 36 cancers in 185 countries, CA Cancer J. Clin. 68 (6) (2018) 394–424.

[2] M. Orditura, G. Galizia, V. Sforza, V. Gambardella, A. Fabozzi, M.M. Laterza, F. Andreozzi, J. Ventriglia, B. Savastano, A. Mabilia, E. Lieto, F. Ciardiello, F. De Vita, Treatment of gastric cancer, World J. Gastroenterol. 20 (7) (2014) 1635–1649.

[3] Y. Shi, F. Lan, C. Matson, P. Mulligan, J.R. Whetstine, P.A. Cole, R.A. Casero, Y. Shi, Histone demethylation mediated by the nuclear amine oxidase homolog LSD1, Cell 119 (7) (2004) 941–953.

[4] Y.C. Zheng, J. Ma, Z. Wang, J. Li, B. Jiang, W. Zhou, X. Shi, X. Wang, W. Zhao, H.M. Liu, A systematic review of histone lysine-specific demethylase 1 and its inhibitors, Med. Res. Rev. 35 (5) (2015) 1032–1071.

[5] S.F. Alsaqer, M.M. Tashkandi, V.K. Kartha, Y.T. Yang, Y. Alkheriji, A. Salama, X. Varelas, M. Kukuruzinska, S. Monti, M.V. Bais, Inhibition of LSD1 epigenetically attenuates oral cancer growth and metastasis, Oncotarget 8 (43) (2017) 73372–73386.

[6] A. Maiques-Diaz, T.C. Somervaille, LSD1: biologic roles and therapeutic targeting, Epigenomics 8 (8) (2016) 1103–1116.

[7] A. Hosseini, S. Minucci, A comprehensive review of lysine-specific demethylase 1 and its roles in cancer, Epigenomics 9 (8) (2017) 1123–1142.

[8] A. Maiques-Diaz, G.J. Spencer, J.T. Lynch, F. Ciceri, E.L. Williams, F.M.R. Amaral, D.H. Wiseman, W.J. Harris, Y. Li, S. Sahoo, J.R. Hitchin, D.P. Mould, E.E. Fairweather, B. Waszkowycz, A.M. Jordan, D.L. Smith, T.C.P. Somervaille, Enhancer activation by pharmacologic displacement of LSD1 from GFI1 induces differentiation in acute myeloid leukemia, Cell Rep. 22 (13) (2018) 3641–3659.

[9] W.A. Whyte, S. Bilodeau, D.A. Orlando, H.A. Hoke, G.M. Frampton, C.T. Foster, S.M. Cowley, R.A. Young, Enhancer decommissioning by LSD1 during embryonic stem cell differentiation, Nature 482 (7384) (2012) 221–225.

[10] T. Lin, A. Ponn, X. Hu, B.K. Law, J. Lu, Requirement of the histone demethylase LSD1 in Snai1-mediated transcriptional repression during epithelial-mesenchymal transition, Oncogene 29 (35) (2010) 4896–4904.

[11] S. Ambrosio, A. Ballabio, B. Majello, Histone methyl-transferases and demethylases in the autophagy regulatory network: the emerging role of KDM1A/LSD1 demethylase, Autophagy 15 (2) (2019) 187–196.

[12] Y. Duan, W. Qin, F. Suo, X. Zhai, Y. Guan, X. Wang, Y. Zheng, H. Liu, Design, synthesis and in vitro evaluation of stilbene derivatives as novel LSD1 inhibitors for AML therapy, Bioorg. Med. Chem. 26 (23–24) (2018) 6000–6014.

[13] J.L. Ma, T. Zhang, F.Z. Suo, J. Chang, X.B. Wan, X.J. Feng, Y.C. Zheng, H.M. Liu, Lysine-specific demethylase 1 activation by vitamin B2 attenuates efficacy of apatinib for proliferation and migration of gastric cancer cell MGC-803, J. Cell. Biochem. 119 (6) (2018) 4957–4966.

[14] W. Sheng, M.W. LaFleur, T.H. Nguyen, S. Chen, A. Chakravarthy, J.R. Conway, Y. Li, H. Chen, H. Yang, P.H. Hsu, E.M. Van Allen, G.J. Freeman, D.D. De Carvalho, H.H. He, A.H. Sharpe, Y. Shi, LSD1 ablation stimulates anti-tumor immunity and enables checkpoint blockade, Cell 174 (3) (2018) 549-563.e19.

[15] G. Hutvagner, P.D. Zamore, A microRNA in a multiple-turnover RNAi enzyme complex, Science (New York, N.Y.) 297 (5589) (2002) 2056–2060.

[16] L. Peters, G. Meister, Argonaute proteins: mediators of RNA silencing, Mol. Cell 26 (5) (2007) 611–623.

[17] J. Kim, F. Yao, Z. Xiao, Y. Sun, L. Ma, MicroRNAs and metastasis: small RNAs play big roles, Cancer Metastasis Rev. 37 (1) (2018) 5–15.

[18] Y.S. Lee, A. Dutta, MicroRNAs in cancer, Annu. Rev. Pathol. 4 (2009) 199–227.

[19] L.L. Chen, Z.J. Zhang, Z.B. Yi, J.J. Li, MicroRNA-211-5p suppresses tumour cell proliferation, invasion, migration and metastasis in triple-negative breast cancer by directly targeting SETBP1, Br. J. Cancer 117 (1) (2017) 78–88.

[20] M. Ha, V.N. Kim, Regulation of microRNA biogenesis, Nature reviews, Molecular cell biology 15 (8) (2014) 509–524.

[21] X. Yu, M. Odenthal, J.W. Fries, Exosomes as miRNA carriers: formation-function-Future, Int. J. Mol. Sci. 17 (12) (2016).

[22] L. Milane, A. Singh, G. Mattheolabakis, M. Suresh, M.M. Amiji, Exosome mediated communication within the tumor microenvironment, J. Control. Release 219 (2015) 278–294.

[23] C. Villarroya-Beltri, F. Baixauli, C. Gutierrez-Vazquez, F. Sanchez-Madrid, M. Mittelbrunn, Sorting it out: regulation of exosome loading, Semin. Cancer Biol. 28 (2014) 3–13.

[24] Z. Tang, C. Li, B. Kang, G. Gao, C. Li, Z. Zhang, GEPIA: a web server for cancer and normal gene expression profiling and interactive analyses, Nucleic Acids Res. 45 (W1) (2017) W98–w102.

[25] A. Nagy, A. Lanczky, O. Menyhart, B. Gyorffy, Validation of miRNA prognostic power in hepatocellular carcinoma using expression data of independent datasets, Sci. Rep. 8 (1) (2018) 9227.

[26] Y.C. Zheng, Y.C. Duan, J.L. Ma, R.M. Xu, X. Zi, W.L. Lv, M.M. Wang, X.W. Ye, S. Zhu, D. Mobley, Y.Y. Zhu, J.W. Wang, J.F. Li, Z.R. Wang, W. Zhao, H.M. Liu, Triazole-dithiocarbamate based selective lysine specific demethylase 1 (LSD1) inactivators inhibit gastric cancer cell growth, invasion, and migration, J. Med. Chem. 56 (21) (2013) 8543–8560.

[27] T.X. Lu, M.E. Rothenberg, MicroRNA, J. Allergy Clin. Immunol. 141 (4) (2018) 1202–1207.

[28] K. Jayawardana, S.J. Schramm, V. Tembe, S. Mueller, J.F. Thompson, R.A. Scolyer, G.J. Mann, J. Yang, Identification, Review, and Systematic Cross-Validation of microRNA Prognostic Signatures in Metastatic Melanoma, J. Invest. Dermatol. 136 (1) (2016) 245–254.

[29] K. Specjalski, E. Jassem, MicroRNAs: Potential Biomarkers and Targets of Therapy in Allergic Diseases? Arch. Immunol. Ther. Exp. 67 (4) (2019) 213–223.

[30] J. Wan, X. Ling, B. Peng, G. Ding, miR-142-5p regulates CD4+ T cells in human non-small cell lung cancer through PD-L1 expression via the PTEN pathway, Oncol. Rep. 40 (1) (2018) 272–282.

[31] M. Xia, C.J. Liu, Q. Zhang, A.Y. Guo, GEDS: A Gene Expression Display Server for mRNAs, miRNAs and Proteins, Cells 8 (7) (2019).

[32] N.W. Wong, Y. Chen, S. Chen, X. Wang, OncomiR: an online resource for exploring pan-cancer microRNA dysregulation, Bioinformatics (Oxford, England) 34 (4) (2018) 713–715.

[33] L. Liu, S. Liu, Q. Duan, L. Chen, T. Wu, H. Qian, S. Yang, D. Xin, Z. He, Y. Guo, MicroRNA-142-5p promotes cell growth and migration in renal cell carcinoma by targeting BTG3, Am. J. Transl. Res. 9 (5) (2017) 2394–2402.

[34] V. Agarwal, G.W. Bell, J.W. Nam, D.P. Bartel, Predicting effective microRNA target sites in mammalian mRNAs, eLife 4 (2015).

[35] A. Kozomara, M. Birgaoanu, S. Griffiths-Jones, miRBase: from microRNA sequences to function, Nucleic Acids Res. 47 (D1) (2019) D155–d162.

[36] T. Takeda, N. Hattori, T. Tokuhara, Y. Nishimura, M. Yokoyama, M. Miyake, Adenoviral transduction of MRP-1/CD9 and KAI1/CD82 inhibits lymph node metastasis in orthotopic lung cancer model, Cancer Res. 67 (4) (2007) 1744–1749.

[37] M. Tang, G. Yin, F. Wang, H. Liu, S. Zhou, J. Ni, C. Chen, Y. Zhou, Y. Zhao, Downregulation of CD9 promotes pancreatic cancer growth and metastasis through upregulation of epidermal growth factor on the cell surface, Oncol. Rep. 34 (1) (2015) 350–358.

[38] M. Furuya, H. Kato, N. Nishimura, I. Ishiwata, H. Ikeda, R. Ito, T. Yoshiki, H. Ishikura, Down-regulation of CD9 in human ovarian carcinoma cell might contribute to peritoneal dissemination: morphologic alteration and reduced expression of beta1 integrin subsets, Cancer Res. 65 (7) (2005) 2617–2625.

[39] O. Barreiro, M. Yanez-Mo, M. Sala-Valdes, M.D. Gutierrez-Lopez, S. Ovalle, A. Higginbottom, P.N. Monk, C. Cabanas, F. Sanchez-Madrid, Endothelial tetraspanin microdomains regulate leukocyte firm adhesion during extravasation, Blood 105 (7) (2005) 2852–2861.

[40] M. Ono, K. Handa, S. Sonnino, D.A. Withers, H. Nagai, S.-i. Hakomori, GM3 ganglioside inhibits CD9-Facilitated haptotactic cell motility: coexpression of GM3 and CD9 is essential in the downregulation of tumor cell motility and malignancy, Biochemistry 40 (21) (2001) 6414–6421.

[41] A. Becker, B.K. Thakur, J.M. Weiss, H.S. Kim, H. Peinado, D. Lyden, Extracellular vesicles in Cancer: cell-to-Cell mediators of metastasis, Cancer Cell 30 (6) (2016) 836–848.

[42] E.L.A.S. Mager I., X.O. Breakefield, M.J. Wood, Extracellular vesicles: biology and emerging therapeutic opportunities, Nat. Rev. Drug Discov. 12 (5) (2013) 347–357.

[43] S.L.N. Maas, X.O. Breakefield, A.M. Weaver, Extracellular vesicles: unique intercellular delivery vehicles, Trends Cell Biol. 27 (3) (2017) 172–188.

[44] M. Razi, C.E. Futter, Distinct roles for Tsg101 and Hrs in multivesicular body formation and inward vesiculation, Mol. Biol. Cell 17 (8) (2006) 3469–3483.

[45] C.W. Brown, J.J. Amante, P. Chhoy, A.L. Elaimy, H. Liu, L.J. Zhu, C.E. Baer, S.J. Dixon, A.M. Mercurio, Prominin2 drives ferroptosis resistance by stimulating Iron export, Dev. Cell 51 (5) (2019) 575–586 e4.

[46] Q. Fan, L. Yang, X. Zhang, X. Peng, S. Wei, D. Su, Z. Zhai, X. Hua, H. Li, The emerging role of exosome-derived non-coding RNAs in cancer biology, Cancer Lett. 414 (2018) 107–115.

[47] K. Essandoh, L. Yang, X. Wang, W. Huang, D. Qin, J. Hao, Y. Wang, B. Zingarelli, T. Peng, G.-C. Fan, Blockade of exosome generation with GW4869 dampens the sepsis-induced inflammation and cardiac dysfunction, Biochim. Biophys. Acta 1852 (11) (2015) 2362–2371.

[48] I.J. Fidler, M.L. Kripke, The challenge of targeting metastasis, Cancer Metastasis Rev. 34 (4) (2015) 635–641.

[49] P.S. Steeg, Targeting metastasis, Nat. Rev. Cancer 16 (4) (2016) 201–218.

[50] A. Maiques-Diaz, T.C. Somervaille, LSD1: biologic roles and therapeutic targeting, Epigenomics 8 (8) (2016) 1103–1116.

[51] J.W. Højfeldt, K. Agger, K. Helin, Histone lysine demethylases as targets for anticancer therapy, Nature reviews, Drug discovery 12 (12) (2013) 917–930.

[52] Y. Shi, F. Lan, C. Matson, P. Mulligan, J.R. Whetstine, P.A. Cole, R.A. Casero, Y. Shi, Histone demethylation mediated by the nuclear amine oxidase homolog LSD1, Cell 119 (7) (2004) 941–953.

[53] Z.H. Li, X.Q. Liu, P.F. Geng, F.Z. Suo, J.L. Ma, B. Yu, T.Q. Zhao, Z.Q. Zhou, C.X. Huang, Y.C. Zheng, H.M. Liu, Discovery of [1,2,3]Triazolo[4,5-d]pyrimidine derivatives as novel LSD1 inhibitors, ACS Med. Chem. Lett. 8 (4) (2017) 384–389.

[54] Y.C. Duan, Y.Y. Guan, X.Y. Zhai, L.N. Ding, W.P. Qin, D.D. Shen, X.Q. Liu, X.D. Sun, Y.C. Zheng, H.M. Liu, Discovery of resveratrol derivatives as novel LSD1 inhibitors: design, synthesis and their biological evaluation, Eur. J. Med. Chem. 126 (2017) 246–258.

[55] Y.C. Zheng, D.D. Shen, M. Ren, X.Q. Liu, Z.R. Wang, Y. Liu, Q.N. Zhang, L.J. Zhao, L.J. Zhao, J.L. Ma, B. Yu, H.M. Liu, Baicalin, a natural LSD1 inhibitor, Bioorg. Chem. 69 (2016) 129–131.

[56] L.-Y. Ma, Y.-C. Zheng, S.-Q. Wang, B. Wang, Z.-R. Wang, L.-P. Pang, M. Zhang, J.-W. Wang, L. Ding, J. Li, C. Wang, B. Hu, Y. Liu, X.-D. Zhang, J.-J. Wang, Z.-J. Wang, W. Zhao, H.-M. Liu, Design, synthesis, and structure-activity relationship of novel LSD1 inhibitors based on pyrimidine-thiourea hybrids as potent, orally active antitumor agents, J. Med. Chem. 58 (4) (2015) 1705–1716.

[57] A. Vishnoi, S. Rani, MiRNA biogenesis and regulation of diseases: an overview,

Methods Mol. Biol. 1509 (2017) 1–10.
[58] M. Miyake, M. Koyama, M. Seno, S. Ikeyama, Identification of the motility-related protein (MRP-1), recognized by monoclonal antibody M31-15, which inhibits cell motility, J. Exp. Med. 174 (6) (1991) 1347–1354.
[59] S. Ikeyama, M. Koyama, M. Yamaoko, R. Sasada, M. Miyake, Suppression of cell motility and metastasis by transfection with human motility-related protein (MRP-1/CD9) DNA, J. Exp. Med. 177 (5) (1993) 1231–1237.